# Modelling of Neutron Stars

*Robert Chambers and Pau Petit Rosàs*

*10453923 10457059*

School of Physics and Astronomy

University of Manchester

Second year Theory Computing Project

April 2020

## Abstract

The aim of this report is to model a white dwarf and a neutron star using both Newtonian and Tolman-Oppenheimer-Volkov equations. The behaviour of this simulation is tested for different central pressures and inner types of Fermi gases. In addition, a model of how the star would deform under angular velocity is presented and interpreted.

# 1 Introduction

A white dwarf star is the remaining core of a massive star after it has expelled most of its outer mass due to its inability to support the weight of its own gravity once it has run out of nuclear fuel. The remaining core has a mass comparable to that of the Sun but a radius similar to that of the Earth, making it extremely dense. The star is now supported by electron degeneracy pressure rather than the thermal pressure of main sequence stars; a phenomenon explained by the Pauli exclusion principle. If the star has mass higher than $\sim 1.4$ solar masses (called the Chandrasekhar limit for white dwarfs) after it collapses, the final form will be a neutron star. Neutron stars have an approximate radius of 17km making them one of the most dense objects in the universe. The extreme gravity is supported by neutron degeneracy pressure. If the massive of a neutron star exceeds $\sim 2$ solar masses, the neutron degeneracy pressure can no longer support the star and it will collapse into a black whole. This limit is called the Tolman-Oppenheimer-Volkov limit and is the analogue of the Chandrasekhar limit for white dwarfs. The degenerate gas model is the one that we will be exploring in our project. At first we will solve the coupled equations of state and Newtonian structure equations for a static star for pressure and mass as functions of distance from center,$r$. Then a rotating perturbation can be added. This perturbation of the star will remove polar symmetry and distort the star into a spheroid that we can then recreate on a 3D model.

# 2 Theory

## 2.1 Non-Rotating Model

For our model we wanted to find the pressure, $p$, and mass, $M$, of the neutron star as a function of radius, $r$, for a given initial condition on central pressure. The coupled equations (1),(2) can be classically derived for a spherically symmetric gas of isotropic material in gravitational static equilibrium. Equation (3) is energy density in terms of material density according to Einstein's equation from special relativity.

$$\frac{dp}{dr} = -\frac{G\rho(r)M(r)}{r^2} = -\frac{G\epsilon(r)M(r)}{c^2r^2}, \tag{1}$$

$$\frac{dM}{dr} = 4\pi r^2\rho(r) = \frac{4\pi r^2\epsilon(r)}{c^2}, \tag{2}$$

$$\epsilon(r) = \rho(r)c^2. \tag{3}$$

For a purely classically gas these equations would suffice but for special and general relativistic corrections the Tolman-Oppenheimer-Volkov (TOV) equation is required:

$$\frac{dp}{dr} = -\frac{G\epsilon(r)M(r)}{c^2r^2}\left[1+\frac{p(r)}{\epsilon(r)}\right]\left[1+\frac{4\pi r^3\rho(r)}{M(r)c^2}\right]\left[1-\frac{2GM(r)}{c^2r}\right]^{-1}. \tag{4}$$

We assume a Fermi Gas Model which allows us to couple pressure and energy density through the Fermi momentum [1]. The relation $p = K\epsilon^\gamma$ that comes from this model is a polytrope. In

the relativistic limit the exponent, $\gamma$, is $\frac{4}{3}$, and in the non-relativistic limit is $\frac{5}{3}$. The value of $K$ changes for each polytropic equation of state. These are given by:

$$K_{non-rel} = \frac{\hbar^2}{15\pi^2 m_e}\left(\frac{3\pi^2 Z}{A m_N c^2}\right)^{5/3} \tag{5}$$

$$K_{rel} = \frac{\hbar c}{12\pi^2}\left(\frac{3\pi^2 Z}{A m_N c^2}\right)^{4/3} \tag{6}$$

Both $p$ and $\epsilon$ have dimensions of energy density and can be cast into a dimensionless form, as well as mass. We get

$$\frac{d\bar{p}(r)}{dr} = -\frac{\alpha \bar{p}(r)^{\frac{1}{\gamma}}\bar{M}(r)}{r^2}, \tag{1'}$$

$$\frac{d\bar{M}(r)}{dr} = \beta r^2 \bar{p}(r)^{1/\gamma}, \tag{2'}$$

and

$$\frac{d\bar{p}(r)}{dr} = -\frac{-\alpha \bar{M}(r)\bar{p}(r)^{-1/\gamma}}{r^2}\left[1+\bar{p}(r)^{\frac{\gamma-1}{\gamma}}\bar{K}^{1/\gamma}\epsilon_0^{\frac{\gamma-1}{\gamma}}\right]\left[1+\frac{4\pi r^3 \bar{p}(r)\epsilon_0}{\bar{M}(r)M_\odot c^2}\right]\left[1-\frac{2G\bar{M}(r)M_\odot}{c^2 r}\right]^{-1} \tag{4'}$$

where

$$p = \epsilon_0 \bar{p}, \quad \epsilon = \epsilon_0 \bar{\epsilon}, \quad M(r) = M_\odot \bar{M}(r) \tag{7}$$

$$\epsilon_0 = \left[\frac{1}{K}\left(\frac{R_0}{\alpha}\right)^{\gamma}\right]^{1-\gamma} \tag{8}$$

and $R_0 = GM_\odot/c^2 = 1.47$Km. $\alpha$ is a constant given by

$$\alpha = \frac{R_0}{\bar{K}^{1/\gamma}} = \frac{R_0}{(K\epsilon_0^{\gamma-1})^{1/\gamma}}, \tag{9}$$

and

$$\beta = \frac{4\pi\epsilon_0}{M_\odot c^2 \bar{K}^{1/\gamma}} = \frac{4\pi\epsilon_0}{M_\odot c^2 (K\epsilon_0^{\gamma-1})^{1/\gamma}} \tag{10}$$

.

### 2.2 Rotating Perturbation

The equations used in for this model, unless stated otherwise, were taken from S. Chandrasekhar's paper "The Equilibrium of Distorted Polytropes" [2]. The article thoroughly derives all these equations but for the sake of brevity the pertinent equations have been given as follows. Again, a polytropic equation of state is assumed:

$$P = K\rho^{1+\frac{1}{n}} \tag{11}$$

Density is then written in the form

$$\rho = \lambda \Theta^n, \tag{12}$$

where $\lambda$ is a constant and $\Theta$ is given by a Taylor expansion. By neglecting second and higher order terms Chandrasekhar's finds the following equality

$$\Theta = \theta + v\left[\psi_0(\xi) - \frac{5}{6}\frac{{\xi_1}^2}{3\psi_2(\xi_1) + \xi_1\psi_2'(\xi_1)}\psi_2(\xi)P_2(\mu)\right], \tag{13}$$

where $\theta$, $v$, $\psi_{0,2}$, $\xi$ are as given in the following equations. $P_2(\mu)$ is the second Legendre polynomial with variable, $\mu$, being the cosine of the polar angle measured from the axis of rotation. $\xi$ is the variable used in place of $r$ for the rest of the model and is given by the relation

$$r = \left[\frac{(n+1)K}{4\pi G}\lambda^{\frac{1}{n}-1}\right]^{1/2}\xi, \tag{14}$$

$\theta$ is the solution to the Lane-Emden differential equation

$$\frac{1}{\xi^2}\frac{d}{d\xi}\left(\xi^2\frac{d\theta}{d\xi}\right) = -\theta^n. \tag{15}$$

$\xi_1$ is the radius of the non-rotating star and, consequently, the first zero of Lane-Emden equation. $v$ is a function of angular velocity, $\omega$:

$$v = \frac{\omega^2}{2\pi G\lambda}. \tag{16}$$

$\psi_{0,2}$ are the solutions to the differential equations

$$\frac{1}{\xi^2}\frac{d}{d\xi}\left(\xi^2\frac{d\psi_0}{d\xi}\right) = -n\theta^{n-1}\psi_0 + 1, \tag{17}$$

$$\frac{1}{\xi^2}\frac{d}{d\xi}\left(\xi^2\frac{d\psi_0}{d\xi}\right) = \left(-n\theta^{n-1} + \frac{6}{\xi^2}\right)\psi_2. \tag{18}$$

In order to apply the RK4 numerical method, equations (15), (17), (18) were transformed using the substitution

$$\Gamma = \xi\theta, \tag{19}$$

$$\eta_{0,2} = \xi\psi_{0,2}. \tag{20}$$

Thus, they become

$$\frac{d^2\Gamma}{d\xi^2} = -\xi^{1-n}\Gamma^n, \tag{15'}$$

$$\frac{d^2\eta_0}{d\xi^2} = -n\left(\frac{\Gamma}{\xi}\right)^{n-1}\eta_0 + \xi, \tag{17'}$$

$$\frac{d^2\eta_2}{d\xi^2} = \left(-n\left(\frac{\Gamma}{\xi}\right)^{n-1} + \frac{6}{\xi^2}\right)\eta_2, \tag{18'}$$

further leading to

$$\Theta = \frac{1}{\xi}\left(\Gamma + v\left[\eta_0 - \frac{5}{6}\frac{\xi_1^3\eta_2(\xi)P_2(\mu)}{2\eta_2(\xi_1) + \frac{d\eta_2(\xi_1)}{d\xi}}\right]\right). \tag{13'}$$

Finally, the oblateness, $\sigma$, of the rotating star could be found using

$$\sigma = \frac{5}{4}\frac{v}{|\theta_1'|}\cdot\frac{\xi_1\psi_2(\xi_1)}{3\psi_2(\xi_1) + \xi_1\psi_2'(\xi_1)}, \tag{21}$$

which could then be used to create a 3D model of the spheroid star.

# 3 Methods

## 3.1 The RK4 method

For the non-rotating case we have two coupled ordinary differential equations (1') or (4') and (2'). As there is no analytical solution, we use the Runge-Kutta algorithm to attain a numerical solution [3]. In particular, we have used the Forth Order Runge-Kutta method, which is based, as all other RK methods, on a Taylor expansion. This leads to four equations that allows us to calculate the value of the variable $y$ by increasing the radius $r$ by small steps $h$ with an error proportional to $h^4$.

$$k_1 = f(r_i, y_i), \tag{22}$$

$$k_2 = f(r_i + \frac{h}{2}, y_i + \frac{h}{2}k_i), \tag{23}$$

$$k_3 = f(r_i + \frac{h}{2}, y_i + \frac{h}{2}k_2), \tag{24}$$

$$k_4 = f(r_i + h, y_i + hk_3), \tag{25}$$

$$y_{i+1} = y_i + \frac{h}{6}(k_1 + 2k_2 + 2k_3 + k_4), \tag{26}$$

where

$$f(r, y) = \frac{dy}{dr}. \tag{27}$$

The algorithm is run from the center of the star, where both radius and mass are zero, to the point at which pressure becomes zero (within one step size of $h$). This is where the radius and total mass are found.

For the rotating model we use the same method. This is because, in spite of being able to analytically solve Lane-Emden's equation for $n = 0, 1, 5$ there are no solutions for other $n$. In this case three differential equations (15')(17')(18') are solved. As these are now second order differential equations, the RK4 method had to be applied to both the desired variable and its

first derivative simultaneously. The initial boundary condition is the same as for the non-rotating star, but the algorithm now stops at $\xi_1$. The values of $\eta_{0,2}(\xi_1)$ are found and used to calculate the oblateness.

# 4 Results

## 4.1 Non-Rotating Model

The code outputs Figure 1a) showing how pressure is distributed with distance from the center. This can also be seen for the mass distribution in Figure 1b).

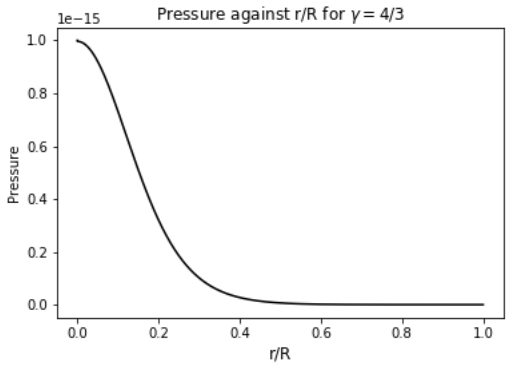


(a)

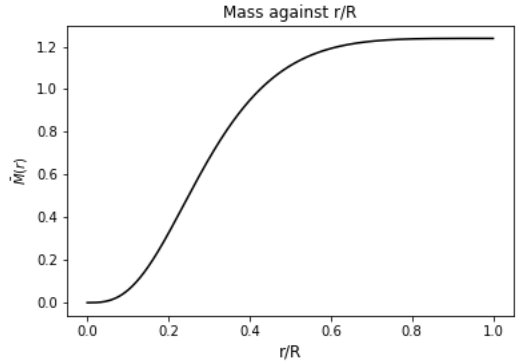


(b)

Figure 1: Pressure (a) and Mass (b) against r/R for $\gamma = \frac{4}{3}$. Initial parameters: $\alpha = 1.473$ Km and $\bar{p}(0) = 10^{-15}$.

A plot of p against r/R for varying values of central pressure, Figure 2b, shows a identical distribution with a linear dependence on central pressure. This suggests that all white dwarfs have the same pressure, and thus mass, distribution as a function of the proportion of their radius, implying the distribution is purely dependent on the EoS in our model. Figure 2a shows that mass distribution is independent of central pressure for white dwarfs with relativistic Fermi gas.

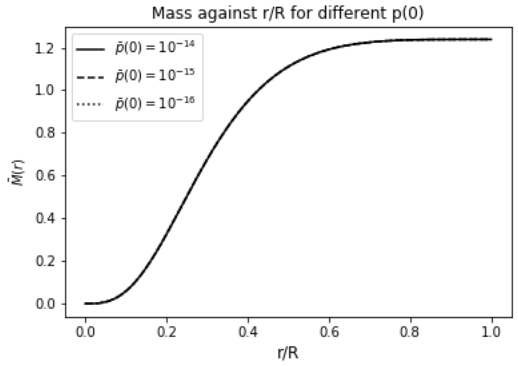


(a)

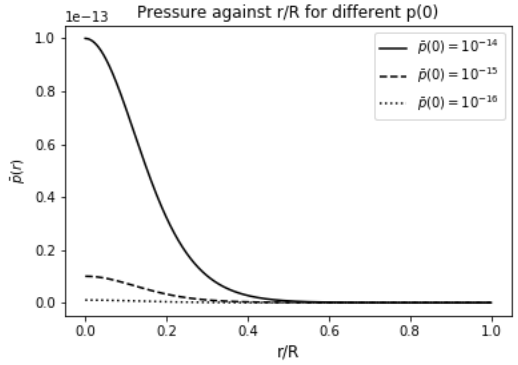


(b) .

Figure 2: Mass (a) and pressure (b) against r/R for the three different central pressures. Initial boundary condition of $\gamma = 4/3, \alpha = 1.473$

In addition, we can see in Figure 3a comparison between the two types of inner Fermi gases. It is noticed that pressure and mass decrease and increase faster for a Fermi relativistic gas. The values of mass are denoted to be much higher for relativistic inner Fermi gas. This agrees with the theory, as non-relativistic white dwarfs must be less energetic, and so less massive.
For neutron stars, Table 1 shows how they behave with and without general relativity corrections, plus compares some dimensionless central pressures.

| $\bar{p}(0)$ | R (Newton) | M (Newton) | R (TOV) | M (TOV) |
|---|---|---|---|---|
| $10^{-4}$ | 14.95 | 0.7 | 13.78 | 0.57 |
| $10^{-5}$ | 18.81 | 0.35 | 18.2 | 0.32 |
| $10^{-6}$ | 23.69 | 0.18 | 23.38 | 0.17 |

Table 1: Radius R (km) and mass $M(M_\odot)$ for neutron stars with $\alpha = 1$km and a non-relativistic Fermi gas.

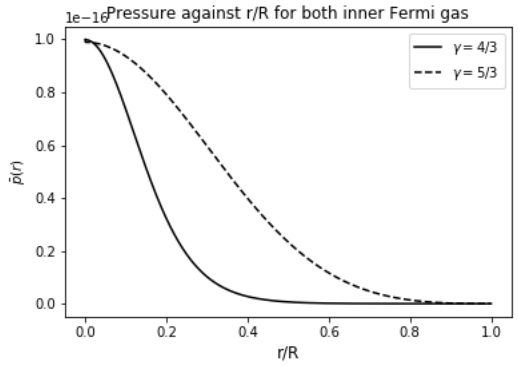


(a)

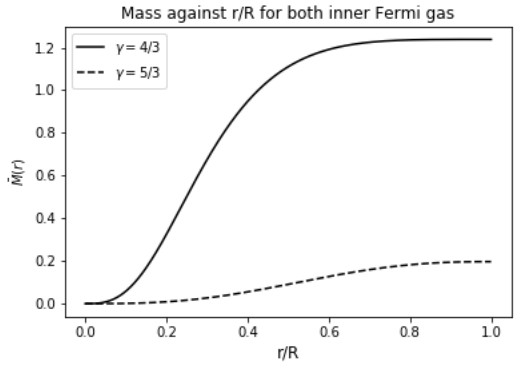


(b) .

Figure 3: Pressure (a) and Mass (b) against r/R for the two types of inner Fermi gas. Initial boundary condition of $\bar{p}(0) = 10^{-16}$

The results indicate that radius gets smaller with general relativity corrections, which is in support of the theory, as Einstein's gravity is stronger than Newton's. Additionally, it is obvious that general relativity corrections are not negligible. Finally, with decreasing central pressure radius increases but mass decreases. Again, this matches the expectations.

### 4.2 Rotating-Perturbation

The rotating perturbation agreed with the static model when angular rotation was set to 0 which implies that both models were functioning correctly.

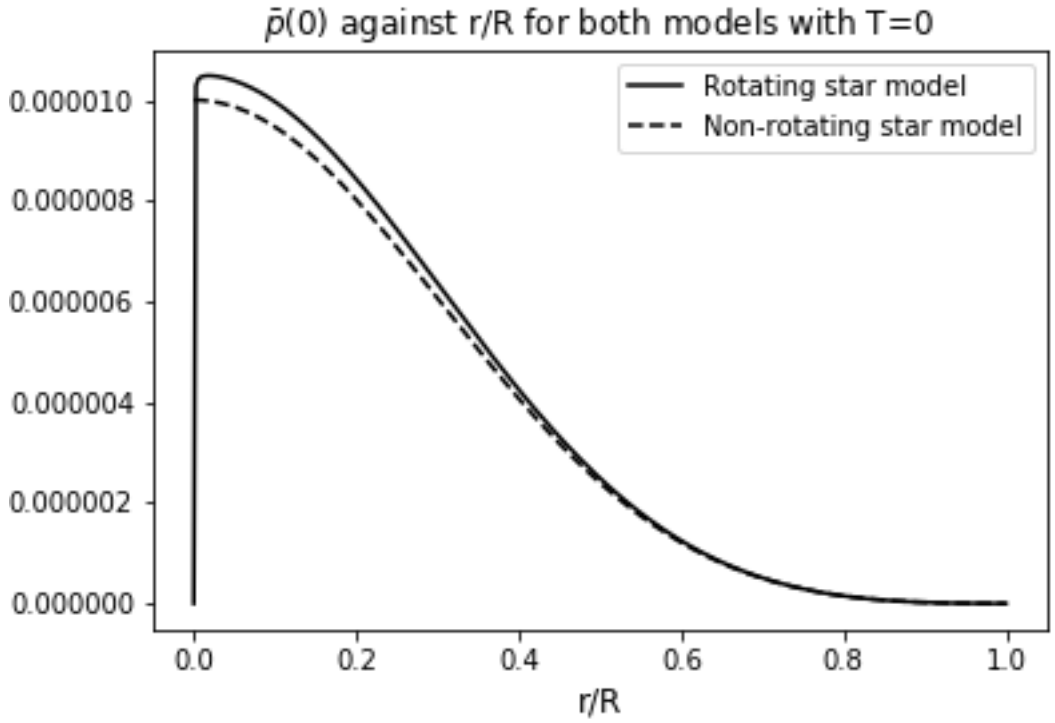


Figure 4: Comparison for both models for a neutron star with $\bar{p}(0) = 10^{-5}$

However for non-zero rotation, once $\xi$ passed the value of $\xi_1$ the values of equations (15')(17')(18') rapidly approached $-\infty$ so they did not allow equation (13') to be implemented beyond the first zero point of the Lain-Emden equation. This means that the pressure and density distributions could not be found in the 'additional regions' beyond the $\xi_1$ sphere, permitted by the change to the Newtonian structure equations. Nevertheless, the shape could still be modelled as the oblateness could be calculated using variables that could be found within the $\xi_1$ sphere.
The model was run for different periods of rotation and was found to break at 1.68 ms, where the oblateness reached 1, as seen in Figure 5. This period turns to be close to 0.33 ms, which is the believed limit for a neutron star of mass $M = 1.442\mathrm{M}_{\odot}$[4].

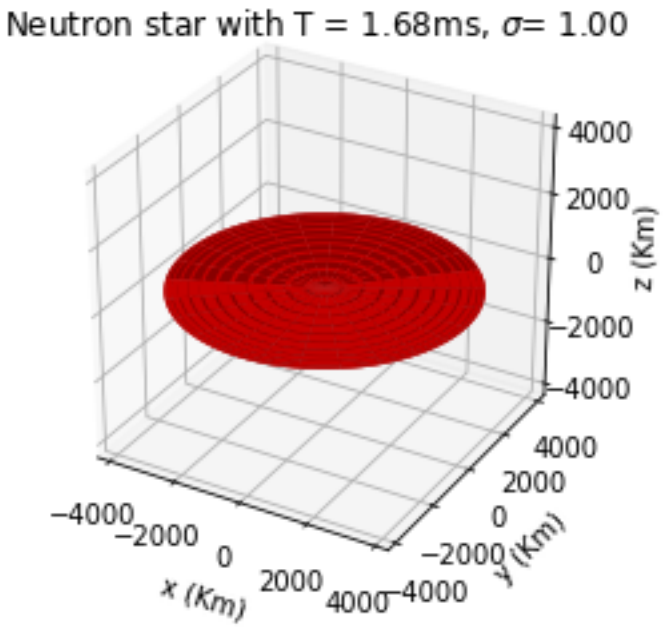


Figure 5: Point at which the neutron star would disintegrate, according to our model. Thus, giving a maximum angular frequency of $\omega = 3740$Hz. This is a limit of our model due to slow rotational approximations made in the derivation of the equations in [2], rather than a physical limit of neutron stars themselves.

In Figure 6 we can observe how the flattening occurs. Again, the theory is satisfied, because with lower period (higher angular velocity) there is, consequently, greater flattening.

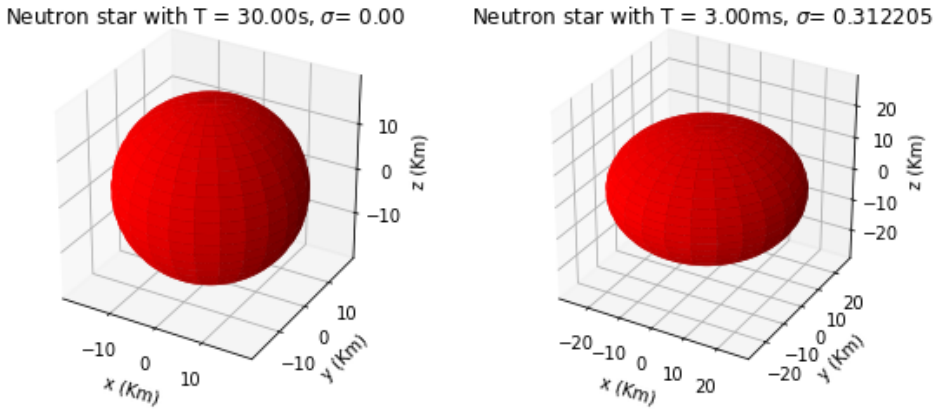


(a) Neutron star with T = 30 s (b) Neutron star with T = 3 ms

Figure 6: Comparison on how an increase in angular velocity affects the neutron star. Sub figure a) has equatorial radius R = 18.7 Km and b) has R = 27.2 Km.

## 5 Conclusions

Many approximations and simplifications were made to our model in order to make the equations easily integrable. The first of these was an idealistic equation of state: assuming an ideal Fermi gas and an isotropic, spherically (or cylindrically, in the rotating case) symmetric distribution. We also assumed that this polytropic equation for the gas was applicable for all densities throughout the star, whereas the equation of state would change through the star as the density decreases towards the edge. Furthermore, for the rotating stars we have dismissed second and higher order terms in $v = \dfrac{\omega^2}{2\pi G\lambda}$, as the model works better for small velocities and just used newtonian physics. Starting by generalizing the rotating model for general relativity loads of things can be done to go one step further. Nevertheless, the model for both rotating and non-rotating stars appears to be consistent with the theory and, even though it has its limitations, it is a close description of reality. Finally, it would be interesting to apply the rotating model to white dwarfs and see how they behave under rotation, comparing them with neutron stars.

## References

[1] Richard R. Silbar and Sanjay Reddy. "Neutron stars for undergraduates". In: *American Journal of Physics* 72.7 (2004), pp. 892–905. DOI: 10.1119/1.1703544. eprint: https://doi.org/10.1119/1.1703544. URL: https://doi.org/10.1119/1.1703544.

[2] S. Chandrasekhar and E. A. Milne. "The Equilibrium of Distorted Polytropes: (I). The Rotational Problem". In: *Monthly Notices of the Royal Astronomical Society* 93.5 (Mar. 1933), pp. 390–406. ISSN: 0035-8711. DOI: 10.1093/mnras/93.5.390. eprint: https:

//academic.oup.com/mnras/article-pdf/93/5/390/2793671/mnras93-0390.pdf. URL: https://doi.org/10.1093/mnras/93.5.390.

[3] M. Hjorth-Jensen. *Computational Physics*. URL: https://courses.physics.ucsd.edu/2017/Spring/physics142/Lectures/Lecture17/Hjorth-JensenLectures2010.pdf.

[4] Norman K.. Glendenn2222221 ing. "Limiting rotational period of neutron stars". In: *Physical Review D* 46.10 (Nov. 1992), pp. 4161–4168.